LncPrep + 96kb inhibits ovarian fibrosis by upregulating prolyl oligopeptidase expression

HONGDAN ZHANG[1,2*], JING WANG[1*], JIANWEI LIU[1], XIANG FAN[1], YINUO JIA[1], YINGTONG HUANG[1], QIHUI HAN[1], SHIMENG WANG[1], LI XIAO[1], XIANG LI[1] and CHUNPING ZHANG[1]

[1]School of Basic Medical Sciences, Jiangxi Medical College, Nanchang University, Nanchang, Jiangxi 330019, P.R. China; [2]Department of Pathology, The Second Affiliated Hospital of Army Medical University, Chongqing 400000, P.R. China

Received September 18, 2024; Accepted February 13, 2025

DOI: 10.3892/mmr.2025.13478

Abstract. LncPrep + 96kb is a long non-coding RNA expressed in murine granulosa cells. The 2.2-kb fragment of lncPrep + 96kb inhibits aromatase expression and estrogen secretion in ovarian granulosa cells. In the present study, lncPrep + 96kb-knockout (KO) mice were generated, and significant ovarian fibrosis and reduced female fertility through fertility monitoring and superovulation. The augmentation of ovarian fibrosis was observed by Sirius red staining and western blot and *RT-qPCR*. Notably, lncPrep + 96kb was identified in conserved non-coding sequences adjacent to the prolyl oligopeptidase (POP) gene. Furthermore, POP expression was shown to be reduced in lncPrep + 96kb-KO mice, whereas overexpression of lncPrep + 96kb increased POP expression. Further studies revealed that POP regulated the expression levels of factors related to fibrosis, including matrix metalloproteinase 2 (MMP2), transforming growth factor β1 (TGF-β1) and peroxisome proliferator activated receptor γ (PPAR-γ). In conclusion, ovarian fibrosis was elevated in lncPrep + 96kb-KO mice, and POP may act as a target of lncPrep + 96kb, which mediates ovarian fibrosis through the regulation of PPAR-γ, MMP2 and TGF-β1 expression.

Introduction

The ovary is a female reproductive organ with key functions including the production of mature eggs and the secretion of steroid hormones (1). Follicles serve as the fundamental functional unit of the ovary and are comprised of oocytes surrounded by theca and granulosa cells (2). Follicles are classified into primordial, primary, secondary, antral and preovulatory follicles based on their developmental stage. Follicular growth begins with the transformation of flattened pregranular cells into cuboidal granulosa cells; these cells undergo continuous proliferation, causing follicles to expand from a single layer to multiple layers. As the antrum forms, granulosa cells differentiate into two subsets: Cumulus cells, which attach to the oocytes; and mural granulosa cells, which adhere to the follicular wall. The cumulus cells enclose oocytes to form the cumulus-oocyte complex (3). Notably, most follicles do not reach maturity, undergoing follicular atresia instead. Only a few follicles reach full maturity, migrate to the ovarian surface, and ovulate successfully (4).

The extracellular matrix (ECM), which comprises collagen, laminin and fibronectin, serves a critical role in follicle development (5-7). Notably, the ECM binds to growth factors and hormones, regulating the growth of granulosa cells and oocytes, in addition to providing structural support for growing follicles (8). During ovulation, luteinizing hormone surges trigger follicular rupture, cumulus expansion and oocyte maturation, with ECM remodeling being key to these processes (9). The inability to synthesize ECM components can lead to sterility or reduced fertility (10). Thus, the cyclical remodeling and degradation of the ECM are essential for follicle formation, maturation and ovulation.

In recent years, the pathological changes associated with ovarian fibrosis have garnered attention. With aging, excessive ECM accumulation in the ovarian microenvironment can induce fibrosis, contributing to ovarian aging (11). Factors such as surgery, inflammation and immune system disorders can also cause ovarian injury (12,13). During ovarian repair, cytokine interactions promote ECM production, leading to fibrosis and impaired ovarian function (14,15). Ovarian fibrosis exacerbates inflammation, disrupts angiogenesis and destabilizes ovarian homeostasis. Additionally, fibrosis in the ovarian cortex can reduce the populations of stromal cells, causing follicular obstruction, poorer oocyte quality and compromised reproductive outcomes (16). Ovarian fibrosis is also linked to various disorders, including endometriomas, polycystic ovary syndrome (PCOS) and premature ovarian failure (POF), ultimately decreasing or depleting ovarian

Correspondence to: Professor Chunping Zhang, School of Basic Medical Sciences, Jiangxi Medical College, Nanchang University, 461 Bayi Street, Nanchang, Jiangxi 330019, P.R. China
E-mail: zhangchunping@ncu.edu.cn

*Contributed equally

Key words: lncPrep + 96kb, ovarian fibrosis, prolyl oligopeptidase, transforming growth factor β1, matrix metalloproteinase 2, peroxisome proliferator activated receptor γ

function (17-22). Consequently, a fibrosis-induced decline in ovarian function poses a serious threat to reproductive health and overall quality of life.

Long non-coding RNAs (lncRNAs) were once considered 'noise' in gene transcription; however, it has been shown that they serve notable roles in both physiological and pathological cellular processes as components of the gene regulatory network (23). With advancements in high-throughput technology, numerous lncRNAs have been identified in mammalian ovarian somatic cells. Despite this, only a few lncRNAs have been thoroughly investigated, and revealed to be involved in follicular development and the regulation of female fertility (24). For example, lncRNA NEAT1, which is highly expressed in mammalian follicles, has been reported to be essential for the formation of the corpus luteum and normal fertility in mice (25). Another lncRNA, FDNCR, has been shown to be primarily expressed in the ovaries of Hu sheep with low proliferation capacity, and can induce granulosa cell apoptosis through the microRNA-543-3p/DCN axis (26). In addition, a previous study suggested that lncRNAs have a crucial role in ECM remodeling, with abnormal expression being closely linked to tissue fibrosis (27). Furthermore, lncRNA MEG3 promotes cardiac fibrosis by inhibiting matrix metalloproteinase 2 (MMP2) expression (28). LncRNA Erbb4-ir mediates transforming growth factor β1 (TGF-β1)-induced renal fibrosis (29) and lncRNA H19X is a key factor in TGF-β-driven fibrosis (30). Additionally, lncRNA PICSAR induces abnormal fibroblast proliferation, excessive ECM deposition and the formation of hypertrophic scarring through the regulation of TGF-β1 (31). LncRNAs also contribute to tumor metastasis by regulating ECM remodeling (32).

Previous studies have highlighted the role of lncRNAs in ovarian follicle development, with dysregulated expression being closely linked to disorders characterized by abnormal follicular growth (33-35). Matsubara *et al* (36) identified lncPrep + 96kb within conserved non-coding sequences adjacent to prolyl oligopeptidase (POP). Notably, lncPrep + 96kb has two transcripts, 2.2kb and 2.8kb, which are specifically expressed in mouse ovarian granulosa cells; however, their function remains unclear. LncPrep + 96kb is a lncRNA that exhibits high expression in mouse granulosa cells. Using *in situ* hybridization, we analyzed the spatial and temporal specific expression of lncPrep + 96kb, revealing that lncPrep + 96kb is predominantly localized in the granulosa cells of primary and secondary follicles (37). Moreover, it has been shown to suppress aromatase expression and estradiol production in granulosa cells by inducing the translocation of endothelial differentiation-associated factor 1 (EDF1) from the nucleus to the cytoplasm (37). The present study successfully generated lncPrep + 96kb-knockout (KO) mice.. The aim of the present study was to investigate the effects and underlying mechanisms of lncPrep + 96kb on ovarian fibrosis.

Materials and methods

Animals. A total of eight lncPrep + 96kb-KO mice were obtained from GemPharmatech Co., Ltd (cat. no. AB849013, C57BL/6J, female mice, 20-25 g, 30 day old, GemPharmatech Co., Ltd). All animals were housed at the Laboratory Animal Center of the Medical College of Nanchang University (Nanchang, China) under controlled conditions, including a stable temperature of 22±2˚C, relative humidity of 50±10% and a 12-h light/dark cycle, and free access to sufficient food and water. All animal care and procedures were approved by the Experimental Animal Center at Nanchang University (approval no. NCULAE-202209280023).

Genotyping. Genotyping of mice was performed using PCR amplification (2 X EasyTaq PCR SuperMix(+dye), cat. no. AS111-11, TransGen Biotech Co., Ltd.) of genomic DNA extracted from tail biopsies. Genotyping was performed using the following primers: LncPrep + 96kb wild-type (WT) mice, forward 5'-GGTAATCCTAACGCCACG-3' and reverse 5'-TACCGAGGCACAGTTTCCA-3'; lncPrep + 96kb-KO mice, forward 5'-GACACGCCTATTCATACAAGG C-3' and reverse 5'-GCAAGCGAGTCAGATTTGGCTTAG AAG-3'. Thermocycling conditions were as follows: 94˚C for 10 min, followed by 36 cycles of 94˚C for 30 s, 55˚C for 45 s, and 65˚C for 45 s, with a final extension at 65˚C for 10 min. PCR products were separated on a 2% agarose gel (cat. no. BKM-AG-100, Shenzhen Bikamei Biotechnology Co., Ltd.) with 1 X Green fluorescent nucleic acid dye (10000X) (cat. no. G8140, Beijing Solarbio Science & Technology Co., Ltd.), and visualized under UV light. Wild-type mice showed a single band at 344 bp, while heterozygous mice showed bands at 390 bp and 344 bp, and homozygous mice showed a single band at 390 bp (Fig. S1)

Assessing female fertility for 6 months. Six female mice aged 21 days, both WT and KO female mice, were randomly selected. The body weight of the female mice was recorded every three days for a total of five times (Fig. S2). The female mice were mated with 12 proven fertile male mice (C57BL/6J, 20-25 g, 21 day old, Changsha Tianqin Biotechnology Co., Ltd.) at a 1:1 ratio. Successful mating was confirmed by the presence of a vaginal plug. After natural delivery, the pregnancy rate and the number of offspring were recorded.

Superovulation. Superovulation was induced in KO and WT female mice through intraperitoneal injection of 10 IU pregnant mare serum gonadotropin (PMSG; cat. no. P9970; Beijing Solarbio Science & Technology Co., Ltd.), followed by an additional 10 IU human chorionic gonadotropin (cat. no. YZ-150555; Beijing Solarbio Science & Technology Co., Ltd.) injection 48 h later. The mice were euthanized by cervical dislocation 13 h after the second injection. Subsequently, the ampulla of the fallopian tube was dissected under a stereomicroscope to collect and count oocytes for further analysis.

Hematoxylin and eosin (H&E) staining. The ovarian tissue were extracted from KO and WT mice and fixed in 4% paraformaldehyde (cat. no. P1110; Beijing Solarbio Science & Technology Co., Ltd.) at room temperature for 24 h and then embedded in paraffin. Subsequently, 3-4-μm sections were prepared, followed by dewaxing and hydration. Using a H&E Staining Kit (cat. no. G1121; Beijing Solarbio Science & Technology Co., Ltd.), the nuclei were stained with hematoxylin for 15 sec and the cytoplasm was stained with eosin at room temperature for 30 sec. Finally, dehydration, clarification, neutral gum sealing and light microscopic observation were carried out sequentially.

Sirius-Red staining. Ovarian tissue sections (5 μm) were deparaffinized and stained using the Sirius-Red Staining solution (cat. no. G1472; Beijing Solarbio Science & Technology Co., Ltd.) according to the manufacturer's instructions at room temperature for 24 h. The slices were then immersed in xylene and alcohol and mounted with synthetic resin. Three images from different fields of view were randomly selected for each tissue section, and images were captured using a light microscope (magnification, x10). The images were exported in JPG format with a resolution of 1,920x1,080 pixels via NDP.view2 (Hamamatsu Photonics K.K.). ImageJ (National Institutes of Health) was used to select areas and collagen fiber content was semi-quantified by calculating the ratio of staining intensity in the selected area to the total staining intensity of the ovarian tissue.

Plasmid construction. PCDNA3.0-lncPrep + 96kb 2.2kb and PCDNA3.0-lncPrep + 96kb 2.8kb plasmids (37), and a pMigR1-POP plasmid (18) were constructed as previously described. The lncPrep + 96kb 2.2kb and 2.8kb sequences were amplified by PCR and inserted into the PCDNA 3.0 vector (cat. no. V79020, Thermo Fisher Scientific Inc.) following restriction enzyme digestion with *Kpn*I (cat. no. R3142M; New England BioLabs, Inc.) and *Eco*RI (cat. no. R3101V; New England BioLabs, Inc.). A guide RNA (gRNA) targeting lncPrep + 96kb was cloned into the pSpCas9(BB)-2A-GFP vector (PX458) (cat. no. 48138, Addgene, Inc.). The PX458 plasmid was digested with *Bbs*I and then annealed to the gRNA, and successful insertion was confirmed by Sanger sequencing. PCR primer sequences for lncPrep + 96kb 2.2kb were: Forward, 5'-TTGGTACCAGCTTGTGTATTGCTCATAT-3' and reverse, 5'-GGAATTCTTTGCTTTTTAATTTTTATTTG-3'; and the sequences for lncPrep + 96kb 2.8kb were: Forward, 5'-AGATCATGACAGGGGCTCCT-3' and reverse, 5'-AGCTGGCTGGTCCTCACAG-3'.

To construct the pMigR1-POP plasmid, the entire sequence of POP was amplified and digested with *Xho*I (cat. no. R0146V; New England BioLabs, Inc.) and *Eco*RI, and were subsequently cloned into the pMig plasmid vector (cat. no. MZ0431, Shanghai Qiming Biotechnology Co., Ltd.). The successful insertion was confirmed through Sanger sequencing. PCR primer sequences for POP were: Forward, 5'-CCGCTCGAGATGCTGTCCTTCCAGTACCC-3' and reverse, 5'-CCGGAATTCTTACTGGATCCACTCGATGTT-3'.

Granulosa cell culture and transfection. A total of six female mice (C57BL/6J, 25-30 g, 21 day old, Changsha Tianqin Biotechnology Co., Ltd.) were injected with 5 IU PMSG. After 48 h, the mice were euthanized by cervical dislocation and their ovaries were harvested. The ovaries were then placed in petri dishes containing sterile PBS (cat. no. P1020; Beijing Solarbio Science & Technology Co., Ltd.) and follicles were mechanically punctured with an injection needle to release granulosa cells. The PBS containing granulosa cells was collected in a centrifuge tube (cat. no. UFC910096; Merck KGaA) and centrifuged at 2,500 x g for 5 min at room temperature. After discarding the supernatant, the cells were cultured in DMEM/F12 (cat. no. D6501, Beijing Solarbio Science & Technology Co.; Ltd.), 1% penicillin-streptomycin (cat. no. FG101-01, TransGen Biotech Co., Ltd.,) in a 6-well culture plate (cat. no. CFE-F1006-01; TransGen Biotech Co., Ltd.,) at 37˚C in a humidified atmosphere of 5% CO_2. Once cell confluence reached 70-80%, the cells were transfected with 2 μg plasmid using FuGENE® 6 Transfection Reagent (cat. no. E2691; Promega Corporation). After 8 h at 37˚C, the medium was replaced with fresh medium. The cells underwent RNA and protein extraction 48 h post-transfection, and the effects of plasmid transfection were verified using reverse transcription-quantitative polymerase chain reaction (RT-qPCR) and western blotting (WB) (Fig. S3).

RT-qPCR. RNA was extracted from granulosa cells or ovarian tissue using TransZol UP Enhanced RNA extraction kit (cat. no. ET111-01-V2; TransGen Biotech Co., Ltd.), and its concentration was measured using a NanoDrop 2000 spectrophotometer (Thermo Fisher Scientific, Inc.). RT was performed using the RT Kit (cat. no. AE311; TransGen Biotech Co., Ltd.;) according to the manufacturer's protocol. RT was carried out at 42˚C for 30 min, with reverse transcriptase inactivation performed at 85˚C for 5 min. qPCR was conducted using the QuantiNova® SYBR Green PCR Kit (cat. no. 208054; Qiagen GmbH). According to the kit's instructions, the amplification system was prepared and run on a PCR instrument (CFX96 Connect; Bio-Rad Laboratories, Inc.). The reaction conditions were as follows: Initial denaturation step at 95˚C for 5 min, followed by 40 cycles at 60˚C for 10 sec and 95˚C (+0.5˚C/cycle) for 15 sec, and a final step at 95˚C for 15 sec. β-actin was used as an internal control for standardization, and relative quantification was calculated using the $2^{-\Delta\Delta Cq}$ method (38). Primer sequences, supplied by TransGen Biotech Co., Ltd, are listed in Table I.

WB. Ovarian tissue or cells were lysed in RIPA buffer (cat. no. PC101; Shanghai Yamei Biomedical Technology Co., Ltd.,) supplemented with 1X alkaline phosphatase inhibitors 100X (cat. no. P1260; Beijing Solarbio Science & Technology Co., Ltd.) and 1X protease inhibitors 100X (cat. no. P6731; Beijing Solarbio Science & Technology Co., Ltd.). Protein concentration was measured using the Easy II Protein Quantitative (BCA) Kit (cat. no. DQ111-01; TransGen Biotech Co., Ltd). A total of 20 μg/lane protein samples were separated by 12% sodium dodecyl sulfate-polyacrylamide gel electrophoresis and were then transferred to PVDF membranes (pore size, 0.2 μm; cat. no. ISEQ00010; Merck KGaA). The membranes were blocked with Blocker™ BLOTTO TBS solution (cat. no. 37530; Thermo Fisher Scientific, Inc.) for 1 h at room temperature, followed by overnight incubation at 4˚C with primary antibodies. After an incubation with the secondary antibodies at room temperature for 1 h, the protein bands were visualized and semi-quantified using the EasySee Western Blot Kit (cat. no. DW101-01; TransGen Biotech Co., Ltd.) and Image Lab™ software 3.0 (Bio-Rad Laboratories, Inc.).

The following antibodies were used for WB: Anti-PREP/POP (1:1,000; cat. no. A00298-2; Bioworld Technology, Inc.), anti-β-actin (1:5,000; cat. no. 66009-1-Ig; Wuhan Sanying Biotechnology), anti-peroxisome proliferator activated receptor γ (PPAR-γ; 1:1,000; cat. no. BA2120; Boster Biological Technology Co., Ltd.), anti-TGF-β1 (1:500; cat. no. BA0290; Boster Biological Technology), anti-MMP2 (1:1,000; cat. no. A00286; Boster Biological Technology), Mouse anti-Goat IgG (H+L) Cross-Adsorbed Secondary Antibody, HRP (1:20,000; cat. no. HS101; TransGen Biotech

Table I. Oligonucleotides used for RT-qPCR.

Gene	Primer sequence
PPAR-γ	Sense: 5'-AGGACATCCAAGACAACCTG-3' Antisense: 5'-CTCTGTGACAATCTGCCTGA-3'
MMP2	Sense: 5'-GAACACCTTCTATGGCTGC-3' Antisense: 5'-GTTGTAGTTGGCCACATCTG-3'
TGF-β1	Sense: 5'-CCAACTATTGCTTCAGCTCCA-3' Antisense: 5'-TTATGCTGGTTGTACAGGG-3'
β-actin	Sense: 5'-TAAAGACCTCTATGCCAACACAGT-3' Antisense: 5'-CACGATGGAGGGGCCGGACTCATC-3'
POP	Sense: 5'-CCGCTCGAGATGCTGTCCTTCCAGT ACCC-3' Antisense: 5'-CCGGAATTCTTACTGGATCCACTCGAT GTT-3'

PPAR-γ, peroxisome proliferator activated receptor γ; MMP2, matrix metalloproteinase 2; TGF-β1, transforming growth factor β1; POP, prolyl oligopeptidase.

Co., Ltd.), and Rabbit anti-Mouse IgG (H+L) Secondary Antibody, HRP (1:20,000; cat. no. HS201; TransGen Biotech Co., Ltd.).

Statistical analysis. Data were statistically analyzed using GraphPad Prism 7.00 (Dotmatics), and are presented as the mean ± SD. All experiments were repeated at least three times. Differences between two groups were evaluated using an independent samples Student's t-test. One-way ANOVA followed by Student-Newman-Keuls test was used for statistical comparisons among multiple groups. Two-way ANOVA followed by Tukey's HSD test was used to analyze the changes in body weight of mice. $P<0.05$ was considered to indicate a statistically significant difference.

Results

LncPrep + 96kb-KO female mice have decreased fertility. The ovaries serve a crucial role in female reproduction and their abnormal development directly impacts fertility. To investigate the role of lncPrep + 96kb in ovarian function, the fertility of KO and WT mice were assessed. Over 6 months of female fertility testing, KO mice produced significantly fewer pups compared with WT mice (Fig. 1A). No significant differences were observed in body weight changes between the groups (Fig. S2). The number of litters born to KO mice was notably lower than the number born to WT mice (Fig. 1B), and the average litter size was also significantly reduced in the KO group (Fig. 1C). Additionally, the ovulation rate in immature superovulated mice was evaluated, and it was revealed that KO female mice ovulated fewer eggs (22±12) compared with WT female mice (41±21) (Fig. 1D, E).

LncPrep + 96kb-KO mice exhibit obvious ovarian fibrosis. Ovaries from 2-month-old WT and KO mice were subjected to H&E and Sirius-Red staining. H&E staining revealed no notable differences in follicular morphology between the two groups (Fig. 2A). However, Sirius-Red staining highlighted a marked increase in ovarian fibrosis in KO mice compared with that in WT mice (Fig. 2B). To improve the clarity of fibrosis assessment, Sirius-Red staining was performed without hematoxylin counterstaining; the results showed a marked increase in collagen deposition in KO mice (Fig. 2C). Analysis of three randomly selected Sirius-Red staining sections using ImageJ software confirmed a higher collagen fiber content in KO ovaries compared with in WT ovaries (Fig. 2D).

TGF-β1 expression is increased, whereas MMP2 and PPAR-γ expression is decreased in the ovaries of lncPrep + 96kb-KO female mice. Cytokines such as MMP2, TGF-β1 and PPAR-γ are crucial in the development of tissue fibrosis (15,39). To further explore their roles in ovarian fibrosis, mRNA (Fig. 3A) and proteins (Fig. 3B) were extracted from the ovaries of KO and WT mice. The results revealed an upregulation of TGF-β1 expression in KO mice, whereas MMP2 and PPAR-γ expression levels were significantly downregulated.

LncPrep + 96kb promotes POP expression. LncPrep + 96kb has been identified as a lncRNA transcribed from a conserved non-coding sequence of the mouse POP gene, which regulates POP expression in ovarian granulosa cells (36). Our previous study demonstrated that POP serves a role in androgen-induced fibrosis in an animal model of PCOS by regulating TGF-β1 and MMP-2 expression (18). Analyses of both mRNA (Fig. 4A) and protein (Fig. 4B) levels revealed reduced POP expression in the ovaries of lncPrep + 96kb-KO mice. To further confirm this, granulosa cells were isolated, and it was confirmed that the mRNA expression levels of POP were lower in the KO group compared with those in the WT group (Fig. 4C). Conversely, POP expression was significantly increased in granulosa cells transfected with PCDNA3.0-lncPrep + 96kb 2.2kb and 2.8kb plasmids (Fig. 4D and E). These findings indicated that lncPrep + 96kb may modulate POP expression in the ovary.

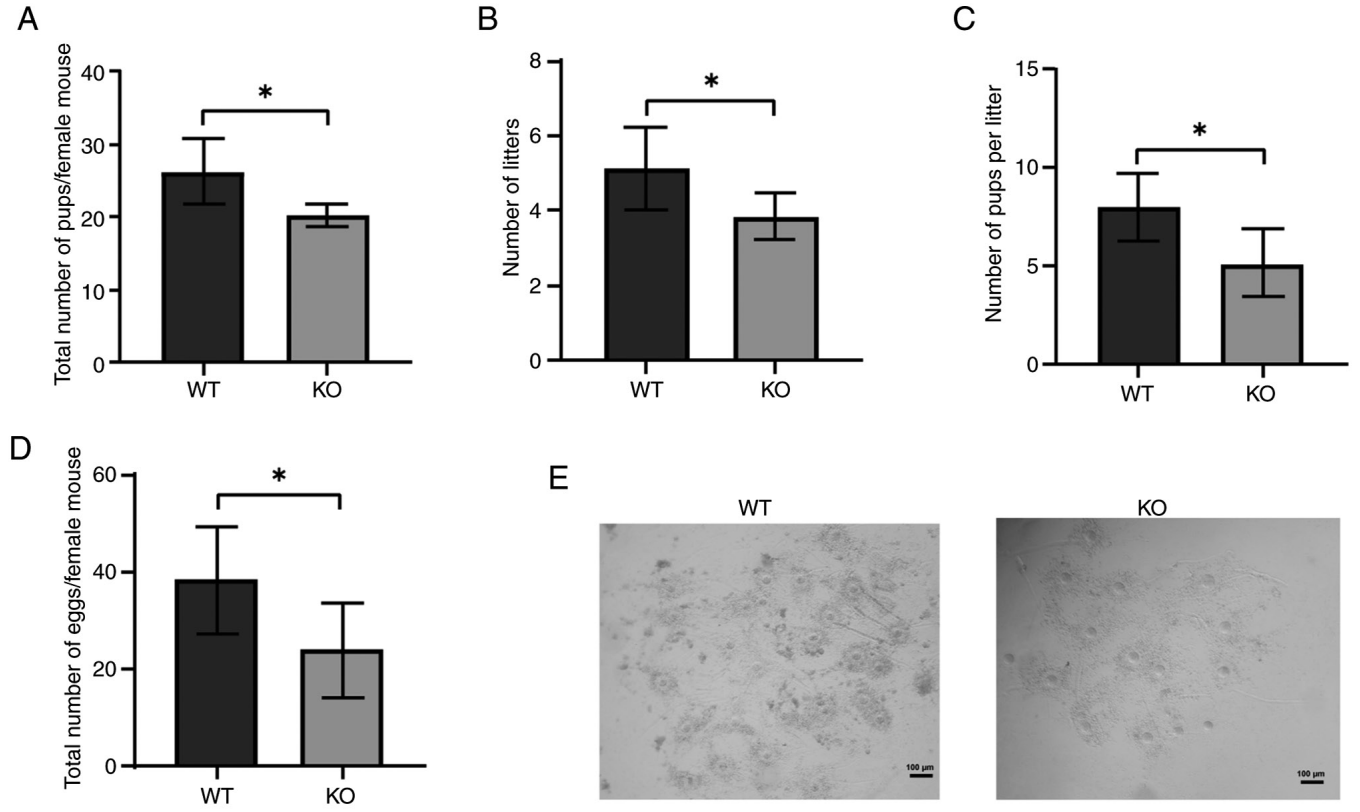

Figure 1. LncPrep + 96kb-KO female mice have decreased fertility. (A) Total number of pups/female mouse. (B) Number of litters, (n=6). (C) Number of pups per litter, (n=6). (D) Total number of eggs/female mouse, (n=3). (E) Egg was inspected under an optical microscope. Scale bar, 100 μm. *P<0.05, as determined by independent samples Student's t-test. KO, knockout; WT, wild-type.

Overexpression of POP inhibits TGF-β1 expression and increases MMP2 and PPAR-γ expression. To further investigate the role of in ovarian fibrosis, granulosa cells were cultured and transfected with the pMigR1-POP plasmid. The results showed that TGF-β1 expression was decreased, and MMP2 and PPAR-γ expression was increased at both the protein (Fig. 5A) and mRNA (Fig. 5B) levels. These findings suggested that POP may modulate the expression of fibrosis-related factors in granulosa cells.

Discussion

Ovarian fibrosis is characterized by the excessive proliferation of ovarian fibroblasts and accumulation of the ECM. Previous studies have shown that various ovarian disorders, including PCOS, ovarian endometriomas and POF, exhibit differing degrees of ovarian fibrosis (40,41). The ovaries of patients with PCOS exhibit abnormally elevated levels of TGF-β1, which promotes ECM production in mesenchymal cells and the synthesis of enzymes that inhibit ECM degradation. This results in excessive ECM accumulation in the ovary, contributing to ovarian interstitial fibrosis (42). Furthermore, systemic and localized chronic low-grade inflammation can increase oxidative stress within the ovary, accelerating the development of ovarian fibrosis (43-46). POF is characterized by fibrous tissue infiltration in the ovarian cortex or stroma and thickening of the ovarian capsule. Zhang *et al* (47) demonstrated that transplantation of human amniotic epithelial cells can inhibit ovarian granulosa cell apoptosis, activate the TGF-β/Smad signaling pathway, and support the restoration of damaged ovarian vascular structures and functionality, thereby improving the symptoms of ovarian fibrosis. The present findings revealed pronounced fibrosis in the ovarian tissues of lncPrep + 96kb-KO mice, suggesting that lncPrep + 96kb may influence ovarian ECM remodeling and thereby affect ovarian function.

The growth, maturation and ovulation of ovarian follicles depend on the cyclical breakdown and restructuring of the ECM. This remodeling process is particularly crucial during cumulus expansion and follicular rupture (48,49). Ovarian fibrosis, marked by excessive ECM deposition, can directly impact follicular development and female fertility (50,51). In the current study, lncPrep + 96kb-KO mice exhibited reduced fertility and ovulation, which may be linked to increased ovarian fibrosis.

The primary pathological features of ovarian fibrosis include increased connective tissue within the mesenchyme, and a reduction or absence of follicles. Research has identified the involvement of various cytokines in the development of tissue fibrosis, including TIMPs, MMPs, ET-1, TGF-β1, VEGF, PPAR-γ and CTGF. These factors interact to disrupt the balance between ECM and degradation, leading to the excessive proliferation of ovarian mesenchymal fibroblasts (15). TGF-β1 serves a critical role in fibrosis by inhibiting MMP expression and activation, upregulating protease inhibitors such as TIMPs and plasminogen activator inhibitors, and promoting ECM component synthesis while suppressing its degradation (52,53). PPAR-γ, a ligand-activated transcription

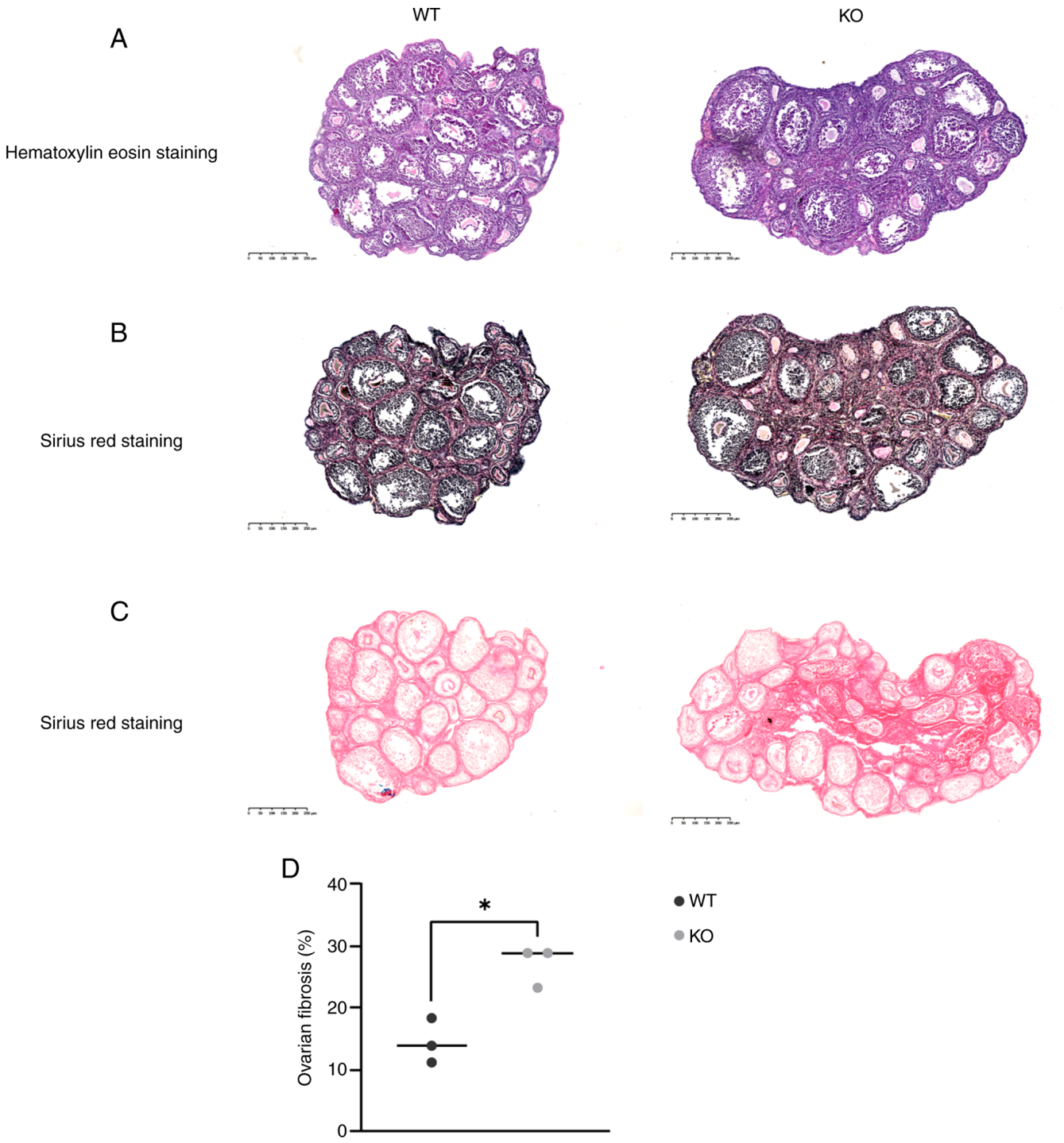

Figure 2. Ovarian fibrosis in lncPrep + 96kb-KO mice. (A) Hematoxylin eosin staining of ovarian sections of 2-month-old mice. Scale bar, 250 μm. (B) Sirius red staining of ovarian sections of 2-month-old mice. (C) Sirius red staining of ovarian sections without hematoxylin counterstaining. Scale bar, 250 μm. (D) Ovarian fibrosis as a percentage of ovarian tissue. Data are presented as the mean ± SD (n=3 mice/group). *P<0.05, as determined by independent samples Student's t-test. KO, knockout; WT, wild-type.

factor, is crucial in regulating glycolipid metabolism, immune system function, cell differentiation and apoptosis, and inflammatory responses. It has been shown that PPAR-γ agonists block TGF-β signaling, thereby impeding the progression of fibrosis (54). By regulating TGF-β and other pathways, PPAR-γ can inhibit the activation and proliferation of hepatic stellate cells, reduce ECM production and exert anti-fibrosis effects (55,56). MMP2 is present in all cell types, and degrades degenerated collagen I, collagen IV and other ECM proteins. In animal models of diabetic cardiomyopathy, reduced MMP2 activity has been shown to be associated with increased myocardial fibrosis (57). Similarly, in the ovary, both endogenous(such as reactive oxygen species and inflammatory mediators) and exogenous (for example, high-fat or high-sugar diets) stimuli can elevate TGF-β1 levels, leading to excessive ECM accumulation, disrupted MMP balance and the promotion of ovarian interstitial fibrosis (15,58,59). Yang *et al* (60) reported that abnormal TGF-β1 expression and follicular fluid

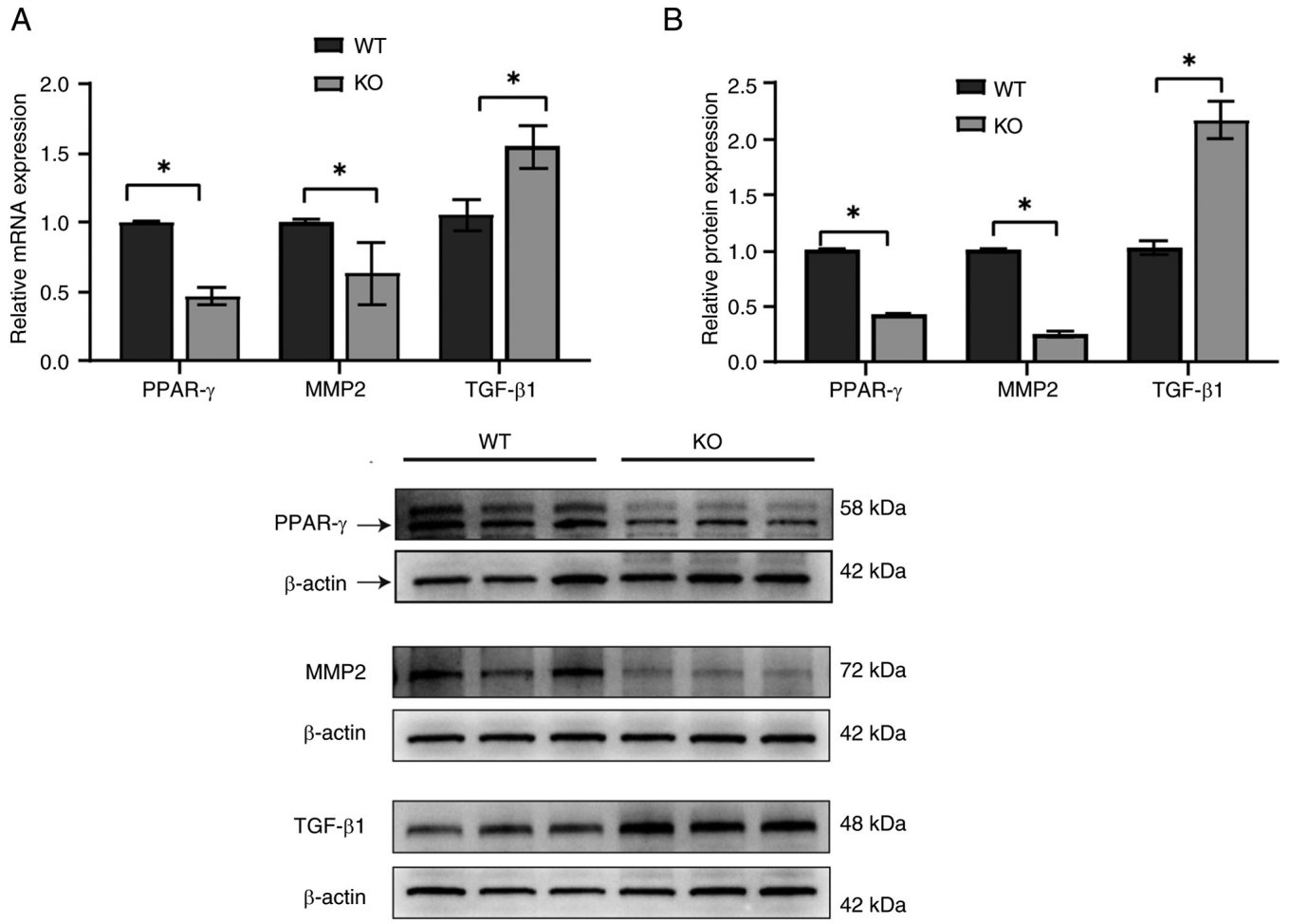

Figure 3. Change in fibrosis-related factors in lncPrep + 96kb-KO mice. (A) mRNA and (B) protein expression levels of TGF-β1, PPAR-γ, and MMP2. *P<0.05, as determined by independent samples Student's t-test. KO, knockout; WT, wild-type; TGF-β1, transforming growth factor β1; MMP2, matrix metalloproteinase 2; PPAR-γ, peroxisome proliferator activated receptor γ.

in patients with PCOS may be closely linked to development of the disease. Furthermore, in animal models of PCOS, the protein levels of TGF-β1 in both the serum and ovarian tissue have been shown to be significantly higher compared with those in the controls (61). According to Miao *et al* (19) rosiglitazone can reduce ovarian fibrosis by lowering TGF-β1 levels in the blood and ovarian tissues of rats with PCOS. In the current study, an increase in TGF-β1 expression was observed in lncPrep + 96kb-KO mice, alongside downregulated PPAR-γ and MMP2 expression. These findings suggested that alterations in these fibrosis-related factors may drive the ovarian fibrosis observed in lncPrep + 96kb-KO mice.

POP is a serine endopeptidase that serves a vital role in physiological processes through its proteolytic activity. Abnormal POP expression has been reported to be associated with Alzheimer's and Parkinson's diseases, and inhibiting of POP is considered a promising strategy for treating neuropsychiatric disorders (62). Cavasin *et al* (63) reported that POP can also participate in the synthesis of the anti-fibrotic peptide N-acetyl-seryl-aspartyl-lysyl-proline (Ac-SDKP); Ac-SDKP inhibits renal fibrosis by suppressing TGF-β signaling (64). Additionally, POP can reduce liver cell activation by blocking the TGF-β signal transduction pathway (65) and inducing PPAR-γ, which offers certain potential for liver fibrosis. The present study demonstrated that POP expression was decreased in the ovaries of lncPrep + 96kb-KO mice, whereas the overexpression of lncPrep + 96kb in granulosa cells promoted POP expression. Given that lncPrep + 96kb is located within a conserved non-coding sequence of the POP gene, it may be hypothesized that POP is the target gene of lncPrep + 96kb. Furthermore, overexpression of POP led to a significant decrease in TGF-β1 expression, coupled with increased levels of MMP2 and PPAR-γ, suggesting that POP may mediate the ovarian fibrosis observed in lncPrep + 96kb-KO mice by regulating the expression levels of TGF-β1, MMP2 and PPAR-γ.

In conclusion, the present study generated lncPrep + 96kb-KO mice and observed that lncPrep + 96kb KO was associated with increased ovarian fibrosis. As a target of lncPrep + 96kb, POP serves a key role in regulating TGF-β1, PPAR-γ and MMP2 expression, contributing to the development of ovarian fibrosis. Despite the progress made in the current study, there are still limitations that need to be addressed. Firstly, the present study focused solely on the regulation of ovarian fibrosis by lncPrep + 96kb via POP; however, ovarian fibrosis is a complex process, and other mechanisms are likely involved. Future research should investigate additional pathways to gain a more comprehensive understanding of the regulatory mechanisms underlying

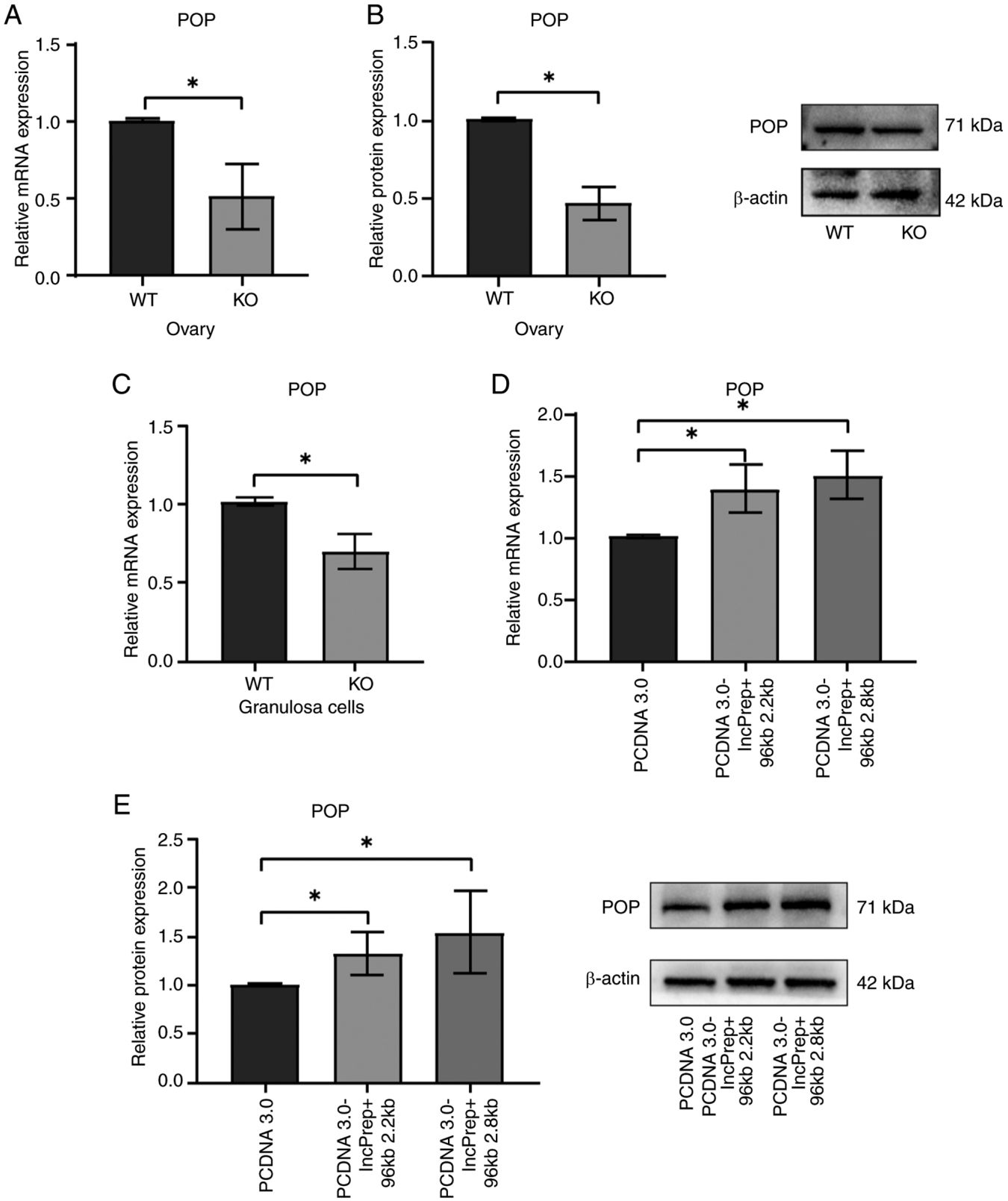

Figure 4. Impact of lncPrep + 96kb on POP expression. (A) mRNA and (B) protein expression levels of POP in the ovaries of mice. (C) mRNA expression levels of POP in granulosa cells. (D) mRNA and (E) protein expression levels of POP following overexpression of lncPrep + 96kb 2.2kb and 2.8kb. *P<0.05, as determined by independent samples Student's t-test or one-way ANOVA followed by Student-Newman-Keuls test. KO, knockout; WT, wild-type; POP, prolyl oligopeptidase.

ovarian fibrosis. Since lncPrep + 96kb exhibits specific expression in granulosa cells and is crucial for follicular development, other mechanisms may also be responsible for the observed reduction in fertility and ovulation. Further studies are needed to investigate how lncPrep + 96kb regulates ovarian function and impacts fertility.

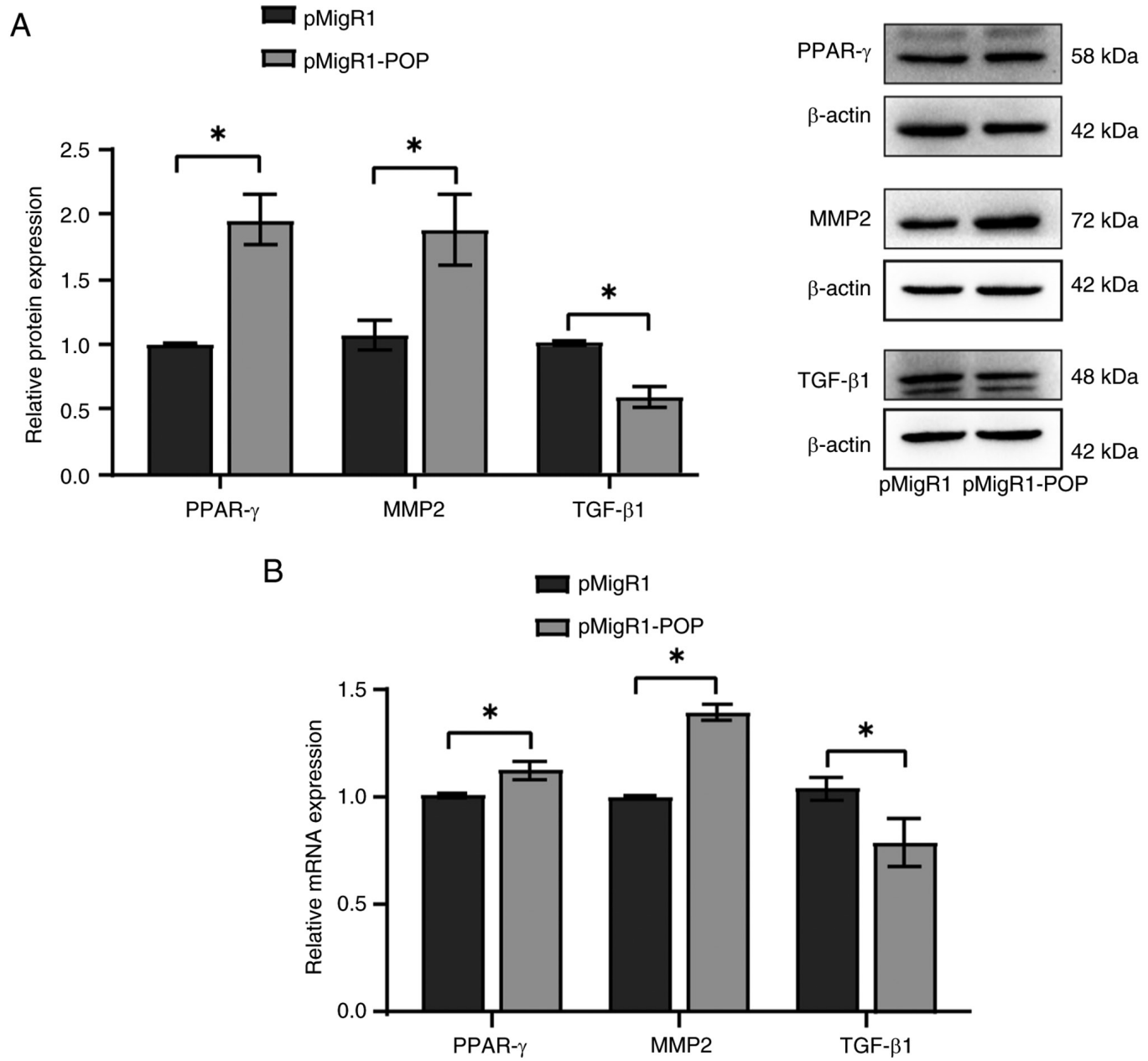

Figure 5. Effects of POP on the regulation of fibrosis-related factors. (A) Protein and (B) mRNA expression levels of PPAR-γ, MMP2 and TGF-β1 following overexpression of POP (pMigR1-POP). *P<0.05, as determined by independent samples Student's t-test. TGF-β1, transforming growth factor β1; MMP2, matrix metalloproteinase 2; PPAR-γ, peroxisome proliferator activated receptor γ; POP, prolyl oligopeptidase.

Acknowledgements

Not applicable.

Funding

This study was funded by the National Natural Science Foundation of China (grant nos. 32160176 and 81960272) and Natural Science Foundation of Jiangxi Province (grant no. 20232BAB206023).

Availability of data and materials

The data generated in the present study may be requested from the corresponding author.

Authors' contributions

HZ, JW and CZ performed the experiments, analyzed the data and wrote the manuscript. XF, LX, YJ and XL analyzed the data. YH, SW and JL performed the experiments. HZ, CZ and QH designed the study and performed experiments. SW, LX and CZ confirm the authenticity of all the raw data. All authors read and approved the final version of the manuscript.

Ethics approval and consent to participate

The present study was approved by the ethics committee at Nanchang University (approval no. NCULAE-202209280023).

Patient consent for publication

Not applicable.

Competing interests

The authors declare that they have no competing interests.

References

1. Wang Y, Chao T, Li Q, He P, Zhang L and Wang J: Metabolomic and transcriptomic analyses reveal the potential mechanisms of dynamic ovarian development in goats during sexual maturation. Int J Mol Sci 25: 9898, 2024.
2. Nayudu PL, Vitt UA, Barrios De Tomasi J, Pancharatna K and Ulloa-Aguirre A: Intact follicle culture: What it can tell us about the roles of FSH glycoforms during follicle development. Reprod Biomed Online 5: 240-253, 2002.
3. Paes VM, Vieira LA, Correia HHV, Sa NAR, Moura AAA, Sales AD, Rodrigues APR, Magalhães-Padilha DM, Santos FW, Apgar GA, *et al*: Effect of heat stress on the survival and development of in vitro cultured bovine preantral follicles and on in vitro maturation of cumulus-oocyte complex. Theriogenology 86: 994-1003, 2016.
4. Dunlop CE and Anderson RA: The regulation and assessment of follicular growth. Scand J Clin Lab Invest Suppl 244: 13-17, 2014.
5. Heeren AM, van Iperen L, Klootwijk DB, de Melo Bernardo A, Roost MS, Gomes Fernandes MM, Louwe LA, Hilders CG, Helmerhorst FM, van der Westerlaken LA, *et al*: Development of the follicular basement membrane during human gametogenesis and early folliculogenesis. BMC Dev Biol 15: 4, 2015.
6. Irving-Rodgers HF, Hummitzsch K, Murdiyarso LS, Bonner WM, Sado Y, Ninomiya Y, Couchman JR, Sorokin LM and Rodgers RJ: Dynamics of extracellular matrix in ovarian follicles and corpora lutea of mice. Cell Tissue Res 339: 613-624, 2010.
7. Irving-Rodgers HF and Rodgers RJ: Extracellular matrix of the developing ovarian follicle. Semin Reprod Med 24: 195-203, 2006.
8. Woodruff TK and Shea LD: The role of the extracellular matrix in ovarian follicle development. Reprod Sci 14: 6-10, 2007.
9. Willis EL, Bridges PJ and Fortune JE: Progesterone receptor and prostaglandins mediate luteinizing hormone-induced changes in messenger RNAs for ADAMTS proteases in theca cells of bovine periovulatory follicles. Mol Reprod Dev 84: 55-66, 2017.
10. Yung Y, Ophir L, Yerushalmi GM, Baum M, Hourvitz A and Maman E: HAS2-AS1 is a novel LH/hCG target gene regulating HAS2 expression and enhancing cumulus cells migration. J Ovarian Res 12: 21, 2019.
11. Xia X, Yang Y, Liu P, Chen L, Dai X, Xue P and Wang Y: The senolytic drug ABT-263 accelerates ovarian aging in older female mice. Sci Rep 14: 23178, 2024.
12. Xue L, Li X, Zhu X, Zhang J, Zhou S, Tang W, Chen D, Chen Y, Dai J, Wu M, *et al*: Carbon tetrachloride exposure induces ovarian damage through oxidative stress and inflammatory mediated ovarian fibrosis. Ecotoxicol Environ Saf 242: 113859, 2022.
13. Yang YF, Cheng SY, Wang YL, Yue ZP, Yu YX, Chen YZ, Wang WK, Xu ZR, Qi ZQ and Liu Y: Accumulated inflammation and fibrosis participate in atrazine induced ovary toxicity in mice. Environ Pollut 360: 124672, 2024.
14. Fujimoto H, Yoshihara M, Rodgers R, Iyoshi S, Mogi K, Miyamoto E, Hayakawa S, Hayashi M, Nomura S, Kitami K, *et al*: Tumor-associated fibrosis: A unique mechanism promoting ovarian cancer metastasis and peritoneal dissemination. Cancer Metastasis Rev 43: 1037-1053, 2024.
15. Zhou F, Shi LB and Zhang SY: Ovarian fibrosis: A phenomenon of concern. Chin Med J (Engl) 130: 365-371, 2017.
16. Isola JVV, Hense JD, Osorio CAP, Biswas S, Alberola-Ila J, Ocañas SR, Schneider A and Stout MB: Reproductive Ageing: Inflammation, immune cells, and cellular senescence in the aging ovary. Reproduction 168: e230499, 2024.
17. Cui L, Bao H, Liu Z, Man X, Liu H, Hou Y, Luo Q, Wang S, Fu Q and Zhang H: hUMSCs regulate the differentiation of ovarian stromal cells via TGF-β1/Smad3 signaling pathway to inhibit ovarian fibrosis to repair ovarian function in POI rats. Stem Cell Res Ther 11: 386, 2020.
18. Han S, Wang S, Fan X, Chen M, Wang X, Huang Y, Zhang H, Ma Y, Wang J and Zhang C: Abnormal expression of prolyl oligopeptidase (POP) and Its catalytic products Ac-SDKP contributes to the ovarian fibrosis change in polycystic ovary syndrome (PCOS) mice. Biomedicines 11: 1927, 2023.
19. Miao ZL, Guo L, Wang YX, Cui R, Yang N, Huang MQ, Qin WB, Chen J, Li HM, Wang ZN and Wei XC: The intervention effect of Rosiglitozone in ovarian fibrosis of PCOS rats. Biomed Environ Sci 25: 46-52, 2012.
20. Wang D, Wang T, Wang R, Zhang X, Wang L, Xiang Z, Zhuang L, Shen S, Wang H, Gao Q and Wang Y: Suppression of p66Shc prevents hyperandrogenism-induced ovarian oxidative stress and fibrosis. J Transl Med 18: 84, 2020.
21. Wang D, Weng Y, Zhang Y, Wang R, Wang T, Zhou J, Shen S, Wang H and Wang Y: Exposure to hyperandrogen drives ovarian dysfunction and fibrosis by activating the NLRP3 inflammasome in mice. Sci Total Environ 745: 141049, 2020.
22. Zhou Y, Lan H, Dong Z, Cao W, Zeng Z and Song JL: Dietary proanthocyanidins alleviated ovarian fibrosis in letrozole-induced polycystic ovary syndrome in rats. J Food Biochem 45: e13723, 2021.
23. Ali T and Grote P: Beyond the RNA-dependent function of LncRNA genes. Elife 9: e60583, 2020.
24. Xu XF, Li J, Cao YX, Chen DW, Zhang ZG, He XJ, Ji DM and Chen BL: Differential expression of long noncoding RNAs in human cumulus cells related to embryo developmental potential: A Microarray Analysis. Reprod Sci 22: 672-678, 2015.
25. Nakagawa S, Shimada M, Yanaka K, Mito M, Arai T, Takahashi E, Fujita Y, Fujimori T, Standaert L, Marine JC and Hirose T: The lncRNA is required for corpus luteum formation and the establishment of pregnancy in a subpopulation of mice. Development 141: 4618-4627, 2014.
26. Du X, Liu L, Li Q, Zhang L, Pan Z and Li Q: NORFA, long intergenic noncoding RNA, maintains sow fertility by inhibiting granulosa cell death. Commun Biol 3: 131, 2020.
27. Yang Z, Jiang S, Shang J, Jiang Y, Dai Y, Xu B, Yu Y, Liang Z and Yang Y: LncRNA: Shedding light on mechanisms and opportunities in fibrosis and aging. Ageing Res Rev 52: 17-31, 2019.
28. Piccoli MT, Gupta SK, Viereck J, Foinquinos A, Samolovac S, Kramer FL, Garg A, Remke J, Zimmer K, Batkai S and Thum T: Inhibition of the cardiac Fibroblast-Enriched lncRNA Meg3 prevents cardiac fibrosis and diastolic dysfunction. Circ Res 121: 575-583, 2017.
29. Feng M, Tang PM, Huang XR, Sun SF, You YK, Xiao J, Lv LL, Xu AP and Lan HY: TGF-β Mediates renal fibrosis via the Smad3-Erbb4-IR long noncoding RNA Axis. Mol Ther 26: 148-161, 2018.
30. Pachera E, Assassi S, Salazar GA, Stellato M, Renoux F, Wunderlin A, Blyszczuk P, Lafyatis R, Kurreeman F, de Vries-Bouwstra J, *et al*: Long noncoding RNA H19X is a key mediator of TGF-β-driven fibrosis. J Clin Invest 130: 4888-4905, 2020.
31. Xu S, Dong W and Shi Y: LncRNA PICSAR binds to miR-485-5p and activates TGF-beta1/Smad to promote abnormal proliferation of hypertrophic scar fibroblasts (HSFs) and excessive deposition of extracellular matrix (ECM). Med Mol Morphol 54: 337-345, 2021.
32. D'Angelo E and Agostini M: Long non-coding RNA and extracellular matrix: The hidden players in cancer-stroma Cross-talk. Noncoding RNA Res 3: 174-177, 2018.
33. Abolghasemi M and Mahjoub S: Long noncoding RNAs as a piece of polycystic ovary syndrome puzzle. Mol Biol Rep 48: 3845-3851, 2021.
34. Tu J, Chen Y, Li Z, Yang H, Chen H and Yu Z: Long non-coding RNAs in ovarian granulosa cells. J Ovarian Res 13: 63, 2020.
35. Tu M, Wu Y, Mu L and Zhang D: Long non-coding RNAs: Novel players in the pathogenesis of polycystic ovary syndrome. Ann Transl Med 9: 173, 2021.
36. Matsubara S, Kurihara M and Kimura AP: A long non-coding RNA transcribed from conserved non-coding sequences contributes to the mouse prolyl oligopeptidase gene activation. J Biochem 155: 243-256, 2014.
37. Feng F, Wang J, Bao R, Li L, Tong X, Han S, Zhang H, Wen W, Xiao L and Zhang C: LncPrep + 96kb 2.2 kb inhibits estradiol secretion from granulosa cells by inducing EDF1 translocation. Front Cell Dev Biol 8: 481, 2020.
38. Livak KJ and Schmittgen TD: Analysis of relative gene expression data using real-time quantitative PCR and the 2(-Delta Delta C(T)) method. Methods 25: 402-408, 2001.

39. Yu Q, Cheng P, Wu J and Guo C: PPARγ/NF-κB and TGF-β1/Smad pathway are involved in the anti-fibrotic effects of levo-tetrahydropalmatine on liver fibrosis. J Cell Mol Med 25: 1645-1660, 2021.
40. Hendrix AO, Hughes CL and Selgrade JF: Modeling endocrine control of the pituitary-ovarian axis: Androgenic influence and chaotic dynamics. Bull Math Biol 76: 136-156, 2014.
41. Landry DA, Vaishnav HT and Vanderhyden BC: The significance of ovarian fibrosis. Oncotarget 11: 4366-4370, 2020.
42. Verrecchia F and Mauviel A: Transforming growth factor-beta and fibrosis. World J Gastroenterol 13: 3056-3062, 2007.
43. Velez LM, Seldin M and Motta AB: Inflammation and reproductive function in women with polycystic ovary syndromedagger. Biol Reprod 104: 1205-1217, 2021.
44. Repaci A, Gambineri A and Pasquali R: The role of low-grade inflammation in the polycystic ovary syndrome. Mol Cell Endocrinol 335: 30-41, 2011.
45. Artimani T, Karimi J, Mehdizadeh M, Yavangi M, Khanlarzadeh E, Ghorbani M, Asadi S and Kheiripour N: Evaluation of pro-oxidant-antioxidant balance (PAB) and its association with inflammatory cytokines in polycystic ovary syndrome (PCOS). Gynecol Endocrinol 34: 148-152, 2018.
46. Xiong YL, Liang XY, Yang X, Li Y and Wei LN: Low-grade chronic inflammation in the peripheral blood and ovaries of women with polycystic ovarian syndrome. Eur J Obstet Gynecol Reprod Biol 159: 148-150, 2011.
47. Zhang Q, Bu S, Sun J, Xu M, Yao X, He K and Lai D: Paracrine effects of human amniotic epithelial cells protect against chemotherapy-induced ovarian damage. Stem Cell Res Ther 8: 270, 2017.
48. Lo BKM, Archibong-Omon A, Ploutarchou P, Day AJ, Milner CM and Williams SA: Oocyte-specific ablation of N- and O-glycans alters cumulus cell signalling and extracellular matrix composition. Reprod Fertil Dev 31: 529-537, 2019.
49. MacDonald JA, Takai Y, Ishihara O, Seki H, Woods DC and Tilly JL: Extracellular matrix signaling activates differentiation of adult ovary-derived oogonial stem cells in a species-specific manner. Fertil Steril 111: 794-805, 2019.
50. Curry TE Jr and Smith MF: Impact of extracellular matrix remodeling on ovulation and the folliculo-luteal transition. Semin Reprod Med 24: 228-241, 2006.
51. Smith MF, McIntush EW, Ricke WA, Kojima FN and Smith GW: Regulation of ovarian extracellular matrix remodelling by metalloproteinases and their tissue inhibitors: Effects on follicular development, ovulation and luteal function. J Reprod Fertil Suppl 54: 367-381, 1999.
52. Gong Y, Liu M, Zhang Q, Li J, Cai H, Ran J, Ma L, Ma Y and Quan S: Lysine acetyltransferase 14 mediates TGF-β-induced fibrosis in ovarian endometrioma via co-operation with serum response factor. J Transl Med 22: 561, 2024.
53. Kwak HJ, Park MJ, Cho H, Park CM, Moon SI, Lee HC, Park IC, Kim MS, Rhee CH and Hong SI: Transforming growth factor-beta1 induces tissue inhibitor of metalloproteinase-1 expression via activation of extracellular signal-regulated kinase and Sp1 in human fibrosarcoma cells. Mol Cancer Res 4: 209-220, 2006.
54. Cho Y, Song MK, Kim DI, Kim MS and Lee K: Adverse outcome pathway-based assessment of pulmonary toxicity from the in vivo mixture of biocides dinotefuran and cetylpyridinium chloride. Heliyon 11: e42134, 2025.
55. Li J, Guo C and Wu J: The agonists of peroxisome Proliferator-activated Receptor-gamma for liver fibrosis. Drug Des Devel Ther 15: 2619-2628, 2021.
56. Zhang F, Kong D, Lu Y and Zheng S: Peroxisome proliferator-activated receptor-gamma as a therapeutic target for hepatic fibrosis: From bench to bedside. Cell Mol Life Sci 70: 259-276, 2013.
57. Van Linthout S, Seeland U, Riad A, Eckhardt O, Hohl M, Dhayat N, Richter U, Fischer JW, Böhm M, Pauschinger M, *et al*: Reduced MMP-2 activity contributes to cardiac fibrosis in experimental diabetic cardiomyopathy. Basic Res Cardiol 103: 319-327, 2008.
58. Liu B, Guan YM and Zheng JH: Elevated serum levels of matrix metalloproteinase-2 in women with polycystic ovarian syndrome. Int J Gynaecol Obstet 96: 204-205, 2007.
59. Wang D, Wang W, Liang Q, He X, Xia Y, Shen S, Wang H, Gao Q and Wang Y: DHEA-induced ovarian hyperfibrosis is mediated by TGF-beta signaling pathway. J Ovarian Res 11: 6, 2018.
60. Yang J, Zhong T, Xiao G, Chen Y, Liu J, Xia C, Du H, Kang X, Lin Y, Guan R, *et al*: Polymorphisms and haplotypes of the TGF-β1 gene are associated with risk of polycystic ovary syndrome in Chinese Han women. Eur J Obstet Gynecol Reprod Biol 186: 1-7, 2015.
61. McIlvenna LC, Altintas A, Patten RK, McAinch AJ, Rodgers RJ, Stepto NK, Barrès R and Moreno-Asso A: Transforming growth factor β1 impairs the transcriptomic response to contraction in myotubes from women with polycystic ovary syndrome. J Physiol 600: 3313-3330, 2022.
62. Babkova K, Korabecny J, Soukup O, Nepovimova E, Jun D and Kuca K: Prolyl oligopeptidase and its role in the organism: Attention to the most promising and clinically relevant inhibitors. Future Med Chem 9: 1015-1038, 2017.
63. Cavasin MA, Rhaleb NE, Yang XP and Carretero OA: Prolyl oligopeptidase is involved in release of the antifibrotic peptide Ac-SDKP. Hypertension 43: 1140-1145, 2004.
64. Mizunuma Y, Kanasaki K, Nitta K, Nakamura Y, Ishigaki Y, Takagaki Y, Kitada M, Li S, Liu H, Li J, *et al*: CD-1db/db mice: A novel type 2 diabetic mouse model with progressive kidney fibrosis. J Diabetes Investig 11: 1470-1481, 2020.
65. Jeukendrup AE, Currell K, Clarke J, Cole J and Blannin AK: Effect of beverage glucose and sodium content on fluid delivery. Nutr Metab (Lond) 6: 9, 2009.